Lightning-generated whistler waves observed by probes on the Communication/Navigation Outage Forecast System satellite at low latitudes

R. H. Holzworth,[1] M. P. McCarthy,[1] R. F. Pfaff,[2] A. R. Jacobson,[1] W. L. Willcockson,[1] and D. E. Rowland[2]

Received 8 October 2010; revised 22 April 2011; accepted 26 April 2011; published 8 June 2011.

[1] Direct evidence is presented for a causal relationship between lightning and strong electric field transients inside equatorial ionospheric density depletions. In fact, these whistler mode plasma waves may be the dominant electric field signal within such depletions. Optical lightning data from the Communication/Navigation Outage Forecast System (C/NOFS) satellite and global lightning location information from the World Wide Lightning Location Network are presented as independent verification that these electric field transients are caused by lightning. The electric field instrument on C/NOFS routinely measures lightning-related electric field wave packets or sferics, associated with simultaneous measurements of optical flashes at all altitudes encountered by the satellite (401–867 km). Lightning-generated whistler waves have abundant access to the topside ionosphere, even close to the magnetic equator.

Citation: Holzworth, R. H., M. P. McCarthy, R. F. Pfaff, A. R. Jacobson, W. L. Willcockson, and D. E. Rowland (2011), Lightning-generated whistler waves observed by probes on the Communication/Navigation Outage Forecast System satellite at low latitudes, *J. Geophys. Res.*, *116*, A06306, doi:10.1029/2010JA016198.

1. Introduction

[2] The direct influence of lightning on the upper atmosphere and ionosphere was initially not predicted to be as strong, nor as pervasive, as we now recognize. *Kelley et al.* [1985] carried out the first rocket-borne ionospheric measurements of vector electric fields over thunderstorms and demonstrated that the lightning pulse amplitude was 2 orders of magnitude larger than those of middle latitude ambient ionospheric electric fields, and as many as 3 orders of magnitude larger compared to the magnitude predicted in the scientific literature [cf. *Park and Dejnakarintra*, 1973]. Subsequent in situ measurements in the upper atmosphere and ionosphere [*Holzworth et al.*, 1985, 1999; *Kelley et al.*, 1990, 1997; *Li et al.*, 1991] have clearly established that the lightning EMP (electromagnetic pulse) results in a strong, upward propagating energy packet that converts to whistler mode plasma waves in the ionosphere. *Li et al.* [1991] found that 87% of all lightning strokes detected by a ground based lightning network [see *Orville et al.*, 1983] within 1000 km of the footprint of an ionospheric rocket payload were detected by the electric field sensors on the rocket. *Holzworth et al.* [1999] showed that rocket payloads in the middle latitude, E and F region ionosphere were likely to detect lightning whistler waves up to 2,500 km distant from the sub track. These authors used a model of magnetospheric plasma to show that ELF waves, emanating from lightning, will propagate well into the outer magnetosphere and even to the magnetopause. Additionally, *Berthelier et al.* [2008] have demonstrated lightning-induced lower hybrid solitary waves and associated ion heating are present in the low-latitude ionosphere within regions of very low ionospheric density.

[3] Lightning has been shown to be associated with strong perturbations in ionospheric electron density called explosive Spread F [*Woodman and Kudeki*, 1984]. In that paper it was shown that radar echoes over a range of altitudes in the ionosphere were observed in one to one correspondence following lightning strokes. The authors interpreted these explosive Spread F events as having been caused by the penetration of lightning electric fields into ionospheric regions with weak or marginal instability. Thus, the lightning electric fields were suggested to have triggered the rapid growth of the wave instability and resulting electron density irregularities from which the radar signal was reflected.

[4] Other authors [*Kelley et al.*, 1984; *Liao et al.*, 1989] have examined the growth of a two-stream or a parametric instability, which could be caused by the lightning induced whistler waves, and in turn could explain the explosive Spread F. These papers used midlatitude ionospheric electric field measurements on rockets [*Kelley et al.*, 1984] or remote sensing by radars at the equator (both papers) to build the theoretical analysis. However, until the present work, there have been few in situ VLF electric field measurements at the equator inside the altitude regimes where spread F or explosive spread F phenomena have been observed.

[1] Earth and Space Sciences, University of Washington, Seattle, Washington, USA.
[2] Laboratory for Space Weather, NASA Goddard Space Flight Center, Greenbelt, Maryland, USA.

0148-0227/11/2010JA016198

[5] In addition to these direct, in situ observations of lightning in the ionosphere, recent measurements from satellites of terrestrial gamma radiation sources [e.g., *Fishman et al.*, 1994; *Smith et al.*, 2005; *Briggs et al.*, 2010] have raised new interest in strong electric field coupling from lightning by demonstrating the influence of the lightning EMP on the upper atmosphere and ionosphere.

[6] This paper introduces the C/NOFS satellite measurements of optical and electric field signals from lightning. We compare these measurements to the global lightning locations provided by the World Wide Lightning Location Network (WWLLN) by examining individual events (strokes) in case studies. We present evidence that lightning often results in large electric field signals colocated with narrow, deep ionospheric density depletions in the equatorial ionosphere.

2. Instrumentation and Data Examples

[7] The C/NOFS satellite was launched in April 2008 into an equatorial low-altitude orbit with 13 degree inclination, apogee of 867 km, and perigee of 401 km, with the primary mission to forecast the presence of ionospheric irregularities that adversely impact communication and navigation systems. The satellite is gyroscopically stabilized (nonspinning) and carries a full complement of plasma and field detectors [see *de La Beaujardière et al.*, 2004]. Particularly relevant to this paper is the Vector Electric Field Investigation (VEFI) which measures the DC and AC electric field (DC to 16 kHz) and a Lightning Detector (LD) which measures the optical lightning power. The Planar Langmuir Probe (PLP) provides a measure of absolute plasma density. Data from these instruments will be presented here to demonstrate the one-to-one nature of the lightning (onboard optical and ground-based WWLLN detections) with the upward propagating VLF whistler waves, even up to more than 800 km altitude, with strong signatures even at latitudes near the magnetic equator.

[8] The electric field instrument uses three orthogonal, double Langmuir probes with 20 m tip-to-tip separations, as discussed by *Pfaff et al.* [2010]. Broadband AC or wave electric field measurements are gathered continuously at 512 samples/s in the nominal mode or at 2048, 4096, or 8192 samples/s in the fast or "campaign" mode. For this paper, we focus on brief periods of data gathered with the burst memory which included electric field data sampled at either 16 kilosamples/s or 32 kilosamples/s.

[9] The Planar Langmuir Probe (PLP) is a dual-disk probe to monitor ionospheric plasma densities. PLP provides low time resolution density inputs for background ionosphere models and high time resolution density irregularity measurements to specify disturbance microphysics.

[10] The optical lightning sensor uses two independent silicon photodiodes (44 mm^2 area each) oriented to look toward the nadir (e.g., toward the earth) with one offset to the north and one to the south. The FOV (field of view) is approximately 10 degrees of longitude by 20 degrees of latitude in both the north and in the south looking directions. The LD broadband input channel gathers optical power from 3 pW to 70 nW over the optical band defined by the silicon photodiodes response of 400 nm to 900 nm. The LD is designed with a passband that eliminates slowly varying optical power below about 0.3 Hz.

[11] The LD has two primary modes for data collection: low time resolution "counts" and continuous data collection in burst mode. In the low time resolution mode, which is available continuously, the instrument samples optical power at seven optical power levels for each photodiode, counting the time each channel is in each of the given power levels. These counts are telemetered every 0.5 s for each of the North and South looking LD detectors. In the burst mode, the optical power level from both the North and South LDs are sampled up to 32 kilosamples/s, along with other VEFI instruments such as the electric field waveforms.

[12] An example of the lightning detector data and simultaneous electric field data is shown in Figure 1 and represents a typical example of the optical and electric fields observed by VEFI during a series of lightning events. These data represent continuous measurements within a 25 s burst that were collected at 617 km near 02:24 LT. Figure 1 (top) shows multiple lightning strokes that are organized in clusters or groups, as is typical for thunderstorm-generated lightning in the troposphere. Figure 1 (bottom) shows groups of upward propagating, VLF whistler mode waves which are also organized into similar groups of multiple sferics. The association of the wave electric field sferics and their optical counterparts is evident. These waves were sampled at 16 kilosamples/s and show wave energy extending to the Nyquist frequency of 8 kHz. The waves have a distinct lower cutoff at the local proton frequency near 350 Hz. Below this frequency, there are copious ion whistlers also associated with the optical flashes and VLF sferics. (Note the spectrogram frequency scale is logarithmic to enhance the visibility of the strong electron whistler mode frequency dispersion as well as the ion mode whistler at the lower frequencies.)

[13] We now focus on a single set of sferics and associated optical flashes using an expanded time scale, as shown in Figure 2. This second example is from a different burst, gathered at 828 km near 03:42 LT, in which the burst mode sampled the electric fields at 32 kilosamples/s. Figure 2 (top) shows the LD broadband optical data reveal three lightning events. The first stroke was also located by the World Wide Lightning Location Network (WWLLN) at a time which was a few milliseconds ahead of the LD stroke time (blue line in Figure 2) at a location a few degrees north of the satellite latitude and longitude point. Figure 2 (middle) is the VEFI electric field waveform gathered simultaneously with these lightning strokes. Figure 2 (bottom) presents these same VLF electric field data in spectrogram form. For this example, the electric field data were sampled at 32 kilosamples/s and show strong electric field waves within the sferic spectra up to the Nyquist frequency of 16 kHz.

[14] In Figure 2, we find the expected delay of 10–20 ms between the optical pulses and the electric field sferics, in exactly the same manner as shown by *Kelley et al.* [1990] and *Holzworth et al.* [1999]. This delay is caused by the propagation time for the whistler mode waves below the electron gyrofrequency, as they propagate through the ionospheric plasma. A careful study of data such as these by *Barnum* [1999] allowed determination of the ionospheric electron density by studying the increasing whistler mode dispersion as the wave packet travels upward through the ionospheric plasma. This dispersion is clearly visible in the spectrogram (Figure 2, bottom) for the leading edge of the sferic.

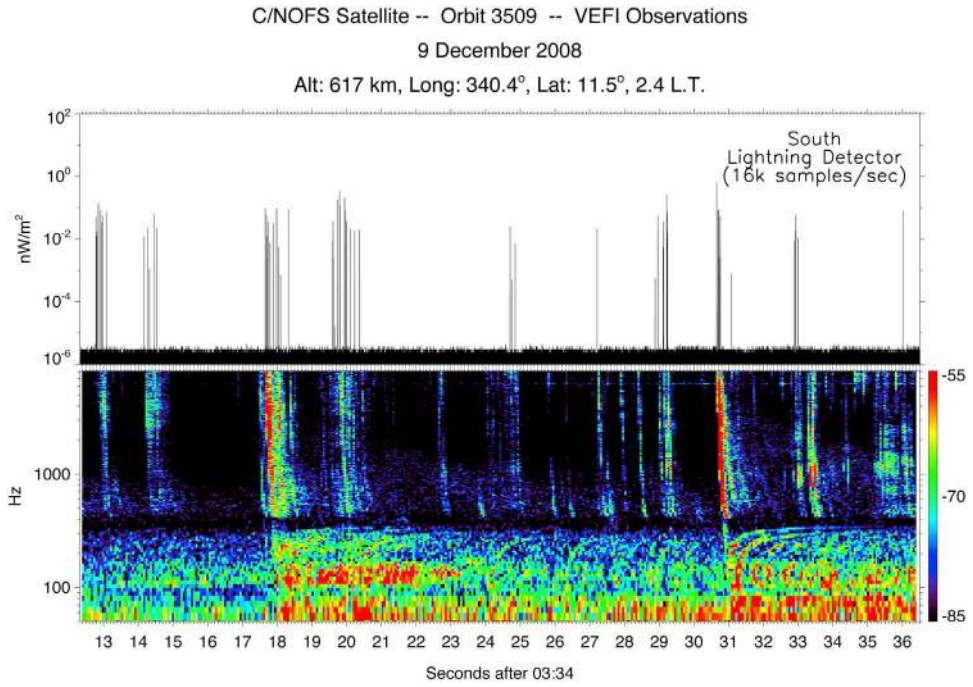

Figure 1. Optical lightning power and VLF electric field spectrogram up to 8 kHz during a sample C/NOFS burst mode collection time.

[15] Also noticeable in Figure 2 (bottom) are the multiple bands of diffuse, plasma waves that extend beyond the stronger, whistler sferics within the VLF band, possibly associated with lower hybrid waves [e.g., *Kelley et al.*, 1985], or with enhanced turbulence caused by nonlinear scattering, as suggested by *Ganguli et al.* [2010]. At this location, we calculate the lower hybrid frequency to be near 10 kHz, since the plasma was ~90% Hydrogen, as determined by the onboard RPA measurements. This might be associated with the diffuse emissions between 10 and 14 kHz, which is just dis-

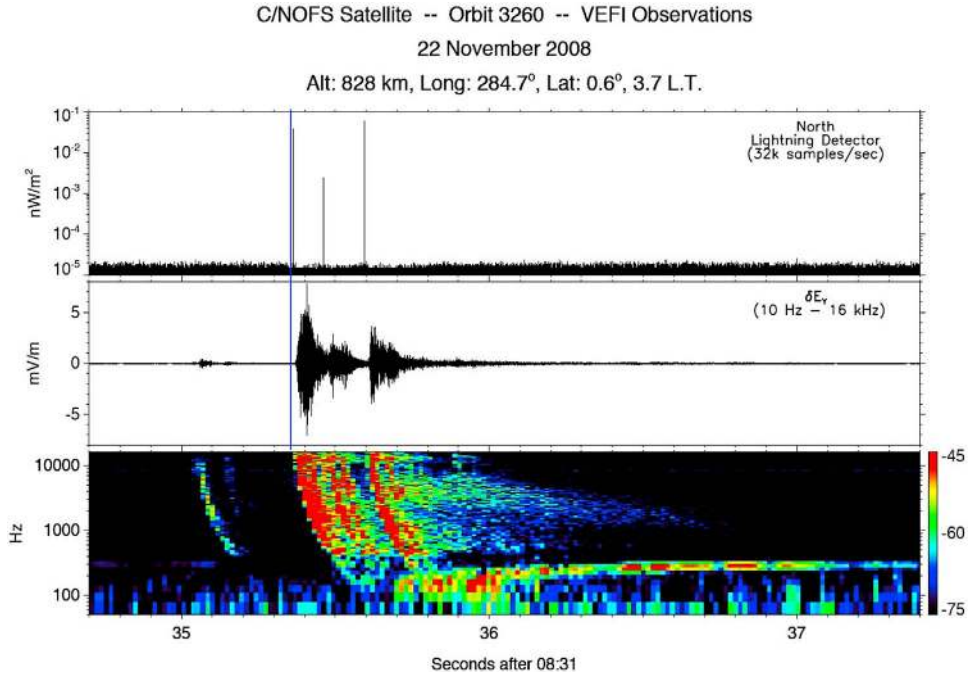

Figure 2. Typical example of isolated lightning events detected in the equatorial ionosphere. Format is the same as Figure 1 except now the (middle) actual electric field waveform is given. Note that the first of three LD optically detected strokes was also located by the WWLLN lightning location network (blue line).

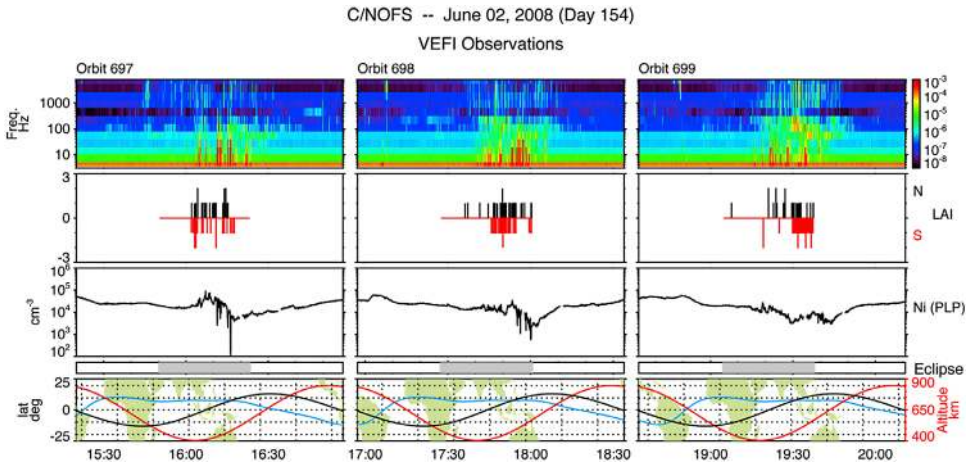

Figure 3. C/NOFS ELF electric field spectrogram (first panel), LD lightning data (second panel), plasma density (third panel), and ephemeris data (fourth panel), showing eclipse periods with shading, along with the altitude and geographic location.

cernible at the top of the spectrogram in Figure 2 (bottom). The data also reveal a second diffuse emission between roughly 2–5 kHz which appears to extend for ~1sec after the last sferic. We note that Figure 2 does not seem to show clear multihop whistlers as have been reported near the equator at the F peak [*Anderson et al.*, 1985].

[16] In addition, the lower-frequency data in Figures 1 and 2 also reveal whistler mode waves that extend up to the hydrogen cyclotron frequency (~300 Hz) which extend for more than a second after the start of these lightning events. Furthermore, these so-called proton whistlers [e.g., *Gurnett et al.*, 1965], evident below the cyclotron frequency of 300 Hz, begin well after the optical lightning flash and at the same time in which the dispersed electron whistler mode energy arrives at the lower (e.g., subcyclotron) frequencies. The ion whistler continues for several seconds, an effect first observed in the ionosphere poleward of 10 degrees latitude by *Gurnett et al.* [1965].

[17] The C/NOFS mission has collected hundreds of high-resolution, burst mode examples similar to Figures 1 and 2, with clear evidence of optical transients from lightning, along with associated dispersed electric field waveforms. These optical and wave signatures are observed at all altitudes encountered by the C/NOFS satellite along its unique, low-latitude orbit described above, despite the fact that the ambient magnetic field lines are nearly horizontal. As the lightning-generated electromagnetic waves enter the ionosphere they are refracted toward the vertical direction (along the ambient density gradient) because of the large index of refraction for VLF whistler mode waves [see *Stix*, 1992]. Although the density gradients are short compared to the wavelengths, it is nevertheless justified to use the quasi-longitudinal (QL) approximation to the Appleton-Hartree equation (as described by *Stix* [1992]) to describe the penetration of these waves into the ionosphere [see *Helliwell*, 1965]. Indeed, the wave vector direction can be up to nearly perpendicular to the magnetic field direction for VLF waves in the Earth's environment. The QL approximation for the index of refraction allows propagation of these whistler mode waves up to very near the resonance cone angle, whose cosine is the ratio of the wave frequency to the electron gyrofrequency [*Stix*, 1992]. For example, within the frequency range considered in this paper, the resonance cone angle would be within 1.5° of perpendicular to the magnetic field direction for 20 kHz waves and even smaller for lower-frequency waves.

[18] So, we might expect these waves at nearly all magnetic latitudes examined by the C/NOFS satellite. However, it is more difficult to account for the short delay times for the dispersion of the whistler mode waves near the equator. For instance, in Figure 2 the delay of the 1 kHz waves from the lightning stroke is on the order of about 10–20 ms, similar to the wave packet delays as a function of frequency seen at higher latitudes [*Holzworth et al.*, 1999]. Within a few degrees of the magnetic equator, the wave vectors are nearly vertical by 400 km altitude [*Helliwell*, 1965]. At, say, 3 degrees from the perpendicular to the magnetic field direction, the index of refraction (N) becomes very large, increasing from N ~50 for a 1 kHz wave at larger angles, to N > 400 within 3 degrees of the vertical. The C/NOFS electric field data may indeed show some examples of such large indices of refraction at times. However, even during times with such large dispersion, the wave measurements are dominated with the much more common short dispersion times (few tens of ms for 1 kHz waves), with dispersions typically <20 even at low magnetic latitude.

[19] The C/NOFS database demonstrates that the low-latitude, nighttime ionosphere between 401 km and 867 km is replete with electric field energy associated with sferics and zero-hop whistlers. This is also where the ionospheric plasma is characterized by deep density depletions associated with irregularities and equatorial spread F. We now investigate how the two phenomena interact.

3. Lightning-Related Electric Fields Within Low-Latitude Density Depletions

[20] We now examine the amplitudes of the lightning-related electric fields in and near plasma density depletions. To motivate our study, Figure 3 shows an example of three consecutive orbits with data from three VEFI instruments: electric field spectrogram from a 12 channel, fixed-frequency filter bank (first panel), LD lightning activity index (second

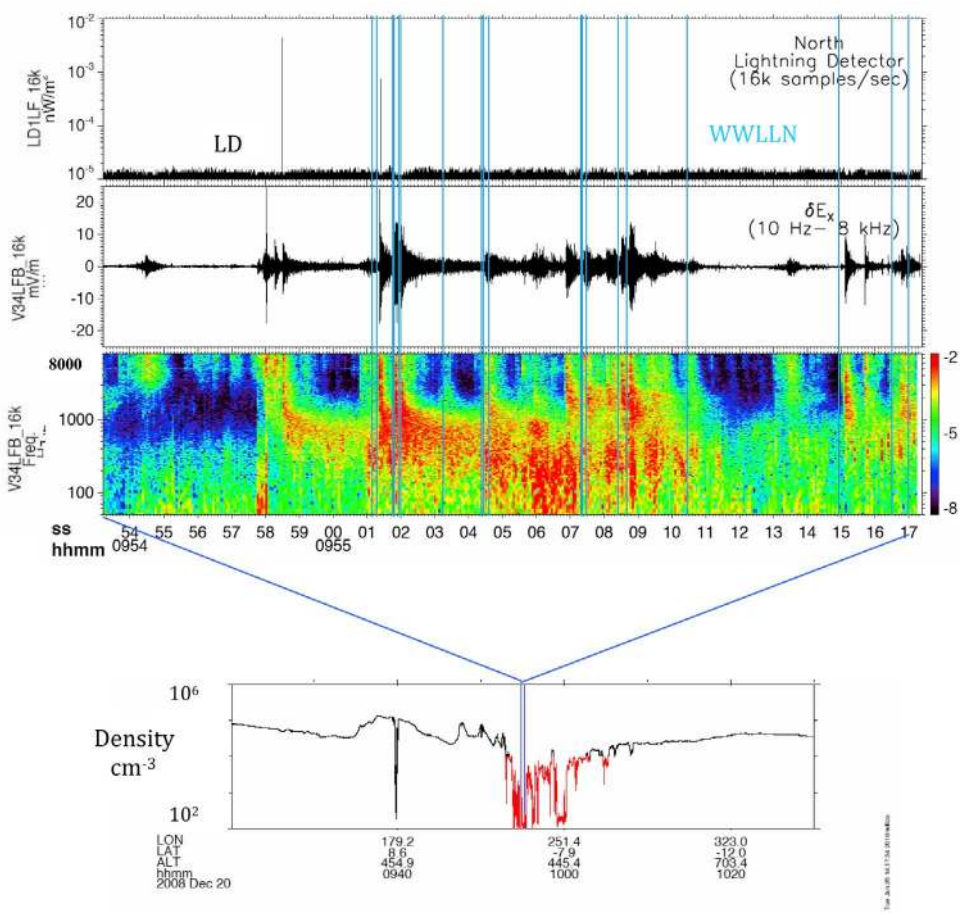

Figure 4. Twenty-four seconds of C/NOFS burst mode data during a deep density depletion. The first panel is the LD lightning data. The second panel is the VLF electric field waveform, along with the third panel down which is a spectrogram of the waveform data in the second panel. The fourth panel in the top portion shows the 16 s/sec plasma density data which reveals the very low plasma density associated with the depletion. The large-scale series of depletions, in which the data in the four panels are embedded, is shown in the plasma density data in the lowest panel.

panel), plasma density (third panel) along with the satellite ephemeris data (Figure 3, bottom), showing eclipse periods, along with the altitude and geographic location. The lightning activity index (LAI) uses the low time resolution north looking (black) and south looking (red) LD data (samples from 7 power levels every 500 ms) and assigns a value of 0–3 depending on the highest level of optical power found during the half-second period (LAI = 0 for no counts at any power level, LAI = 1 for power in LD levels 0 and 1, LAI = 2 for LD power at levels 2–4, and LAI = 3 for counts in any of the top levels 5 or 6). Note the apparent association of enhanced lightning activity with the density perturbations. Note that the optical lightning data are only available for this comparison during eclipse, shown by the horizontal bars. The LAI is intended to present a broad picture of general level of lightning activity every 0.5 s. The LAI data are only plotted when the LD is well within the eclipse period for each orbit, thus the figure says nothing about a relationship between density and lightning outside of the satellite eclipse times. The third panel down is the plasma density from the PLP instrument, and the fourth panel gives the satellite ephemeris information, in which each orbit is centered on local midnight. The eclipse bar shows where the satellite enters eclipse near dusk and exits back to daylight near dawn. Therefore one can see that the eclipse time lightning on these three orbits typically occurred near or after midnight.

[21] There appears to be a broad correlation between the occurrence of the PLP density perturbations or dropouts with the electric field turbulence enhancements (first panel) and with periods of lightning activity (second panel). During these three orbits, all three phenomena (electric field enhancements, density perturbations and lightning) occur during the same time periods around midnight to early morning local times in this particular three orbit sample. Note that local midnight to dawn is not the local time region where one would normally expect either peak lightning or spread F activity. So there is an apparent correlation with both the AC fields (Figure 3, top) and the LD seen in Figure 3 and in many similar C/NOFS data samples. These observations became a stimulus for this detailed study. Only low-resolution data such as shown in Figure 3 does not give a satisfactory proof of time coincidence between the lightning and the electron density because the satellite can detect the lightning remotely but can only detect the density depletions in situ.

[22] To carefully examine the electric fields associated with lightning bursts within density depletions, we collected burst data from the LD and VEFI during deep density depletions. Figure 4 presents a typical burst mode data sample during a deep density depletion. Figure 4 has the first three panels at high time resolution during a burst mode sample. The fourth panel in the set of panels with large time resolution represents the density data at 16 s/sec. The lowest panel shows the overall density perturbation during this orbit and clearly indicates that the burst data were acquired inside one of a series of large plasma depletions. In Figure 4, it can be seen that the large electric field bursts are sferics such as those shown in Figures 1 and 2, although without the characteristic cut off at the proton frequency or clear evidence of proton whistlers. The amplitude of the electric fields is quite large, extending to greater than 10 mV/m.

[23] At first glance, it might appear that the low-frequency, broadband electric field power might be associated with the electrostatic irregularities that are common features of ionospheric density depletions. However, the spectra of such irregularities would include long wavelengths and extend to DC in the satellite frame [e.g., *Kelley*, 2009]. This is the case for the electric fields near 09:54:56 UT which are associated with the plasma gradient, and possibly with the emissions near 09:55:06–07 UT where there is also structure present in the plasma density. The majority of the electric field waves appear to be associated with signatures of sferics. Notice that the electric fields clearly have sharp commencements, exactly as expected for lightning induced electric fields. One interpretation of the extended electric field spectral features between 200 and 1000 Hz would be that associated with the diffuse lower hybrid emissions, as shown in Figure 2. Here, the lower hybrid frequency is considerably lower due to the lower ambient density. Because of the very low density during this burst, RPA data are not available. For reference, for a density of 100/cc and an O+ plasma, the lower hybrid frequency is 521 Hz. This value increases if H^+ plasma is included and also for higher density.

[24] In this example, the optical lightning signature in the C/NOFS data was not pronounced, presumably because many of the lightning flashes occurred outside of the LD field of view. As a result, we have added the flashes from the WWLLN which are shown with blue traces in the first panels. WWLLN detects between 10 and 50% of strokes, depending on energy, so not all VLF lightning wave packets were associated with a located stroke. These traces support a correspondence of the onset of the electric field events with terrestrial lightning strokes. We have examined the C/NOFS burst mode data and have found many similar events during density depletions in which the largest VLF electric field events are clearly associated "one-to-one" with lightning events.

4. Discussion and Summary

[25] In this paper, we have presented a first look at the C/NOFS VEFI/LD optical photodiode instrument. We have demonstrated the expected relationship between optical lightning and the electric field whistlers observed in the electric field data. We find copious numbers of electric field, whistler mode sferics evident at all of the altitudes encountered by C/NOFS (401–867 km) many of which include corresponding optical flashes. The fact that the magnetic field is basically horizontal at these low latitudes would suggest that the whistler mode waves might follow a more complicated path to arrive at the satellite within the low-latitude ionosphere environment. Indeed, the lower-frequency ranges of the spectrum we covered have wavelengths which can be thousands of km, and therefore ray tracing studies may be insufficient, and a full wave analysis such as employed by *Jacobson et al.* [2009] may be required to fully analyze the details of the propagation paths.

[26] Since the C/NOFS satellite location is above the F peak, because of the extremely low solar minimum conditions in which these data were gathered [e.g., *Heelis*, 1999], the fact that the electric field instrument observes such large electric field wave amplitudes suggests that the electric fields may be substantially larger at even lower altitudes. We surmise this conclusion based on the fact that the magnetic field can be expected to redirect the lightning-related electric field energy along the magnetic field direction as the sferic propagates upward.

[27] We then used plasma density data gathered with the C/NOFS Langmuir probe (PLP) to identify periods within the satellite orbit when density depletions occurred and during which lightning-related electric fields were simultaneously detected. The primary scientific conclusion from this analysis is that we find clear times when the largest electric field waves in these density perturbation regions were dominated by the electric field sferics associated with lightning.

[28] The main consequence of the lightning-related electric fields within plasma depletions is that the electric field amplitudes increase considerably due to the changes in the local index of refraction [e.g., *Siefring and Kelley*, 1991] which result in the abrupt reduction in plasma density. As a consequence of this, much larger electric fields are present within the depletion and are available for stimulating secondary instabilities, such as explosive spread F [e.g., *Woodman and Kudeki*, 1984]. The results also show that studies of electric field irregularities within spread F depletions may have significant contributions from whistler mode waves emanating from lightning and thus care must be taken in the interpretation of such electric fields, particularly if only spectral data are available without vector electric and magnetic field waveform observations.

[29] Lightning is not known to be required, nor is it proved here, to be the dominant cause of enhanced density depletions in the equatorial ionosphere, although tropospheric storms have been proposed as a mechanism to seed such depletions [e.g., *McClure et al.*, 1998]. On the other hand, it is our intent here to point out that lightning may be a much more pervasive influence on ionospheric irregularities within density depletions than previously appreciated.

[30] **Acknowledgments.** This analysis at the University of Washington was supported in part by AFOSR grant FA9550-09-1-0309 and in part by NASA grant NNX08AD12G. The authors wish to thank the World Wide Lightning Location Network (http://wwlln.net), a collaboration among over 50 universities and institutions, for providing the lightning location data used in this paper.

[31] Robert Lysak thanks Carl Siefring and another reviewer for their assistance in evaluating this paper.

References

Anderson, D. N., P. M. Kintner, and K. C. Kelley (1985), Inference of equatorial field-line-integrated electron density values using whistlers, *J. Atmos. Terr. Phys.*, *47*(8–10), 989–997, doi:10.1016/0021-9169(85)90078-9.

Barnum, B. (1999), Electromagnetic and optical characteristics of lightning measured in the Earth's ionosphere, Ph.D. thesis, Univ. of Wash., Seattle.

Berthelier, J.-J., et al. (2008), Lightning-induced plasma turbulence and ion heating in equatorial ionospheric depletions, *Nat. Geosci.*, *1*, 101–105, doi:10.1038/ngeo109.

Briggs, M. S., et al. (2010) First results on terrestrial gamma ray flashes from the Fermi Gamma ray Burst Monitor, *J. Geophys. Res.*, *115*, A07323, doi:10.1029/2009JA015242.

de La Beaujardière, O., et al. (2004), C/NOFS: A mission to forecast scintillations, *J. Atmos. Sol. Terr. Phys.*, *66*(17), 1573–1591, doi:10.1016/j.jastp.2004.07.030

Fishman, G. J., et al. (1994), Discovery of intense gamma-ray flashes of atmospheric origin, *Science*, *264*, 1313–1316, doi:10.1126/science.264.5163.1313.

Ganguli, G., L. Rudakov, W. Scales, J. Wang, and M. Mithaiwala (2010), Three dimensional character of whistler turbulence, *Phys. Plasmas*, *17*, 052310, doi:10.1063/1.3420245.

Gurnett, D., S. Shawhan, N. Brice, and R. Smith (1965), Ion Cyclotron Whistlers, *J. Geophys. Res.*, *70*, 1665–1688, doi:10.1029/JZ070i007p01665.

Heelis, R. A. (1999), Ionization layers observed at middle latitudes by Atmosphere Explorer-C, *J. Atmos. Sol. Terr. Phys.*, *61*(5), 407–414, doi:10.1016/S1364-6826(98)00153-9.

Helliwell, R. A. (1965), *Whistlers and Related Ionospheric Phenomena*, Stanford Univ. Press, Stanford, Calif.

Holzworth, R. H., M. C. Kelley, C. L. Siefring, L. C. Hale, and J. D. Mitchell (1985), Electrical measurements in the atmosphere and the ionosphere over an active thunderstorm: 2. Direct current electric fields and conductivity, *J. Geophys. Res.*, *90*, 9824–9830, doi:10.1029/JA090iA10p09824.

Holzworth, R. H., R. M. Winglee, B. H. Barnum, Y. Li, and M. C. Kelley (1999), Lightning whistler waves in the high-latitude magnetosphere, *J. Geophys. Res.*, *104*, 17,369–17,378, doi:10.1029/1999JA900160.

Jacobson, A. R., X.-M. Shao, and R. Holzworth (2009), Full-wave reflection of lightning long-wave radio pulses from the ionospheric *D* region: Numerical model, *J. Geophys. Res.*, *114*, A03303, doi:10.1029/2008JA013642.

Kelley, M. C. (2009), *The Earth's Ionosphere*, 2nd ed., Elsevier, Amsterdam.

Kelley, M. C., D. T. Farley, E. Kudeki, and C. L. Siefring (1984), A model for equatorial explosive spread F, *Geophys. Res. Lett.*, *11*, 1168–1171, doi:10.1029/GL011i012p01168.

Kelley, M. C., C. L. Siefring, R. F. Pfaff, P. M. Kintner, M. Larsen, R. Green, R. H. Holzworth, L. C. Hale, J. D. Mitchell, and D. Le Vine (1985), Electrical measurements in the atmosphere and the ionosphere over an active thunderstorm: 1. Campaign overview and initial ionospheric results, *J. Geophys. Res.*, *90*, 9815–9823, doi:10.1029/JA090iA10p09815.

Kelley, M. C., J. G. Ding, and R. H. Holzworth (1990), Intense ionospheric electric and magnetic field pulses generated by lightning, *Geophys. Res. Lett.*, *17*, 2221–2224, doi:10.1029/GL017i012p02221.

Kelley, M. C., S. D. Baker, R. H. Holzworth, P. Argo, and S. A. Cummer (1997), LF and MF observations of the lightning electromagnetic pulse at ionospheric altitudes, *Geophys. Res. Lett.*, *24*, 1111–1114, doi:10.1029/97GL00991.

Li, Y. Q., R. H. Holzworth, H. Hu, M. McCarthy, R. D. Massey, P. M. Kintner, J. V. Rodrigues, U. S. Inan, and W. C. Armstrong (1991), Anomalous optical events detected by rocket-borne sensor in the WIPP campaign, *J. Geophys. Res.*, *96*, 1315–1326, doi:10.1029/90JA01727.

Liao, C. P., J. P. Freidberg, and M. C. Lee (1989), Explosive spread F caused by lightning-induced electromagnetic effects, *J. Atmos. Terr. Phys.*, *51*(9–10), 751–758, doi:10.1016/0021-9169(89)90032-9.

McClure, J. P., S. Singh, D. K. Bamgboye, F. S. Johnson, and H. Kil (1998), Occurrence of equatorial F region irregularities: Evidence for tropospheric seeding, *J. Geophys. Res.*, *103*(A12), 29,119–29,135, doi:10.1029/98JA02749.

Orville, R. E., et al. (1983), An East Coast lightning detection network, *Bull. Am. Meteorol. Soc.*, *64*(9), 1029–1037, doi:10.1175/1520-0477(1983)064<1029:AECLDN>2.0.CO;2.

Park, G., and M. Dejnakarintra (1973), Penetration of thundercloud electric fields into the ionosphere and magnetosphere: 1. Middle and subauroral latitudes, *J. Geophys. Res.*, *78*, 6623–6633, doi:10.1029/JA078i028p06623.

Pfaff, R., et al. (2010), Observations of DC electric fields in the low-latitude ionosphere and their variations with local time, longitude, and plasma density during extreme solar minimum, *J. Geophys. Res.*, *115*, A12324, doi:10.1029/2010JA016023.

Siefring, C. L., and M. C. Kelley (1991), Analysis of standing wave patterns in VLF transmitter signals: effects of sporadic E layers and in situ measurements of low electron densities, *J. Geophys. Res.*, *96*, 17,813–17,826, doi:10.1029/91JA00615

Smith, D. M., L. I. Lopez, R. P. Lin, and C. P. Barrington-Leigh (2005), Terrestrial gamma-ray flashes observed up to 20 MeV, *Science*, *307*(5712), 1085–1088, doi:10.1126/science.1107466.

Stix, T. H. (1992), *Waves in Plasmas*, Springer, New York.

Woodman, R. F., and E. Kudeki (1984), A causal relationship between lightning and explosive spread F, *Geophys. Res. Lett.*, *11*, 1165–1167, doi:10.1029/GL011i012p01165.

R. H. Holzworth, A. R. Jacobson, M. P. McCarthy, and W. L. Willcockson, Earth and Space Sciences, University of Washington, Seattle, WA 98195-1310, USA. (bobholz@uw.edu)

R. F. Pfaff and D. E. Rowland, Laboratory for Space Weather, NASA Goddard Space Flight Center, Greenbelt, MD 20771, USA.